INVARIANCE THROUGH INFERENCE

Anonymous authors
Paper under double-blind review

ABSTRACT

We introduce a general approach, called Invariance through Inference, for improving the test-time performance of an agent in deployment environments with unknown perceptual variations. Instead of producing invariant visual features through interpolation, invariance through inference turns adaptation at deployment-time into an unsupervised learning problem. This is achieved in practice by deploying a straightforward algorithm that tries to match the distribution of latent features to the agent's prior experience, without relying on paired data. Although simple, we show that this idea leads to surprising improvements on a variety of adaptation scenarios without access to deployment-time rewards, including changes in camera poses and lighting conditions. Results are presented on challenging distractor control suite, a robotics environment with image-based observations.

1 INTRODUCTION

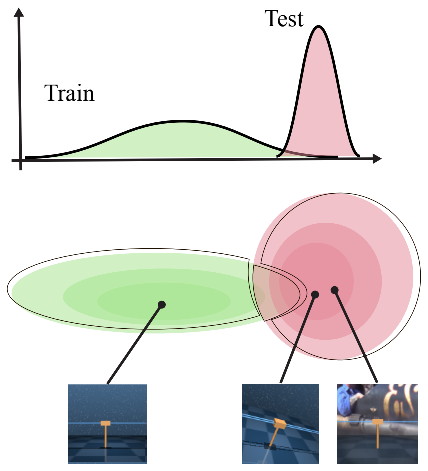

Figure 1: Methods such as data augmentation try to make the training distribution large at the expense of complexity and performance. In spite of these efforts, these methods still often fail to adequately cover the target distribution.

Let us consider the ability of an intelligent agent to generalize to unseen domains. To have such a discussion, we must first consider what generalization means. In much of the learning literature, we typically assume that an agent will accrue experiences of sufficient variation during training, and that these experiences will allow the agent to generalize to novel settings during deployment. Since the richness of the agent's experience is of paramount importance to the quality of its generalization, there exist a broad family of methods that expand the support distribution of the agent's training set. Domain transfer, domain randomization, and meta learning all fall into this category.

Expanding the support of the training distribution is most often accomplished via artificial data augmentation. In pixel-based control tasks, for example, image observations are cropped, shifted, rotated, and discolored to make learned policies more robust to shifts in the input observation at test time (Hansen & Wang, 2020; Yarats et al., 2021). In RL, this type of augmentation can cause value function estimation to become unstable (Laskin et al., 2020; Raileanu et al., 2020; Kumar et al., 2021), and so care must be taken to avoid destabilizing training.

While these approaches are powerful, they are often prone to failure in the case where the target domain is not known *a priori*. In this case, if the target domain falls out-of-distribution, the agent will lack the ability to self correct and will fail, even if great pains were taken to significantly widen the size of its training support. Indeed, as we show in Section 5, even the most robust data augmentation schemes fail when the target observation space differs substantially from that of training. We refer to these approaches *Invariance through Interpolation*, which aims to improve an agent's generalization by increasing the richness of its experiences, as in-distribution generalization.

A more challenging problem—but one that is also more realistic—is generalizing out-of-distribution. In this setting, we assume the specifics of the agent's deployment are not known in advance. Taking this even further, we assume that access to instrumented reward supervision is unavailable in the deployment environment. Here, the burden placed on the agent hoping to generalize is significant. Since we do not have access to reward, fine-tuning via reinforcement learning is impossible. Prior experience will help, but a truly out-of-distribution environment of which the agent has no prior knowledge will make the transfer problem non-trivial. While difficult, this setting of out-of-distribution generalization is nevertheless pervasive in fields such as robotics, wherein a robot trained from pixel observations in the factory will inevitably encounter new settings with different lighting conditions, environmental objects, physical dynamics, and sensor modalities during deployment.

To make progress on out-of-distribution generalization, we consider how we can best leverage the information we do have: the agent's prior experiences during training. Specifically, if we assume the original task the agent was optimized for during training remains well-defined in the target domain, then it is also safe to assume that the agent does have some understanding of the underlying Markov decision process in the target domain. Without further assumptions or loss of generality, we may recast the out-of-distribution generalization problem into an unsupervised adaptation between two MDPs that share underlying dynamics and reward structure, but with distinct observations.

This type of unsupervised adaptation in RL has not been explored widely yet to the best of our knowledge. One of the simplest approaches in this vein is to train a policy with a self-supervised auxiliary task such as inverse dynamics, and rely entirely on it during adaptation (Hansen et al., 2020). Yet attractive for its simplicity, it often performs relatively poorly, as discussed in Section 5. Another approach is to enforce Cycle-GAN (Zhu et al., 2017) style objective to learn cycle-consistent mappings between domains (Zhang et al., 2020). Although it is shown to work well in multiple scenarios, it requires access to states, which is not generally available in pixel-based control tasks we consider.

In this paper, we investigate ways to improve generalization under this challenging scenario. Rather than producing policy invariance by explicitly baking this property into training, we harness probabilistic inference to produce invariance by taking advantage of the latent structure the agent has already discovered in the environment. As we will see, this pays great dividends in producing robotic agents that can function effectively in deployment environments that exhibit different lighting, object texture, or camera poses. To distinguish our approach from prior works that attempt to produce generalization by baking invariances into the policy at training time, we refer to our method as "*Invarivance Through Inference*."

2 Related Work

Generalization in reinforcement learning is a longstanding problem. Recent work has shown that accurately quantifying generalization in this setting poses a challenge (Lee et al., 2019; Cobbe et al., 2019; Zhang et al., 2018). This challenge is further amplified in visual RL from pixels, where measuring the difference between two problems is especially difficult. One promising class of techniques for generalization in image-based RL utilize image augmentation to greatly increase the size of the training distribution. These techniques have enjoyed success in vision research (Chen et al., 2020a; He et al., 2020). However, it was only recently shown that such data augmentation leads to instability in value function estimation in RL algorithms (Hansen & Wang, 2020; Hansen et al., 2021). This line of work showed how to stabilize data-augmented RL, which lead to a significant increase in the generalization capabilities of RL algorithms. The primary shortcoming of these methods is that it is largely impossible to effectively cover the entire potential test distribution by expanding the training distribution, and some test time adaptation is often needed. Several recent works (Hansen et al., 2020; Wang et al., 2020) consider this setting of adaptation at test time, and are further discussed in Section 3.

Invariant Representation Learning is a broad class of techniques for learning representations that are robust across changes in the agent's environment or reward. Often, the agent will use auxiliary information related to dynamics (Hafner et al., 2020) or reward prediction (Jaderberg et al., 2016) to learn a latent representation that is invariant across changing environmental conditions. This is closely related to the idea of **self-supervised learning** (Chen et al., 2020b; Grill et al., 2020).

When applied to visual space RL, it has been shown that self-supervised pre-training provides an efficient way to bootstrap useful invariant representations, even in the absence of a ground-truth reward (Schwarzer et al., 2020; Srinivas et al., 2020).

Domain Shift considers the problem of test-time shift in the underlying input data distribution (Ganin et al., 2016). One common class of techniques for addressing this problem is to learn representations that maximize domain confusion, thus requiring that the agent learn domain-invariant features. This idea has been applied successfully in imitation learning (Stadie et al., 2017). More recent advances have combined Cycle-GANs with imitation learning to produce features that are cycle consistent across domains (Smith et al., 2019). Another approach bottlenecks the information on the latent code of a VAE-based architecture to learn features that are more robust across domain shift in a variety of adversarial settings (Peng et al., 2018).

Meta Learning tries to solve generalization by aggregating learning across distributions of tasks (Finn et al., 2017; Duan et al., 2016; Rakelly et al., 2019). Often, meta learning pipelines focus heavily on fast inference at test time. This is most often accomplished through using some form of bi-level optimization (Rothfuss et al., 2018; Houthooft et al., 2018). Unfortunately, meta learning methods generally require training over entire task distributions. Worse still, this results in the need for a distribution of reward functions for each task during both training and test time. Defining even a single reward function is often quite difficult, let alone many closely related reward functions. Recent work has tried to alleviate this burden with unsupervised training (Hsu et al., 2018).

3 Problem Formulation

Consider the standard infinite horizon Markov decision process (MDP) (Puterman, 2014) parameterized via the tuple $\mathcal{M} = \langle S, O, A, R, P, \gamma \rangle$, where S, O, and A are the state, observation, and action spaces, respectively, $P : S \times A \mapsto S$ is the transition function, $R : S \times A \mapsto \mathbb{R}$ is the scalar reward, and γ is the discount factor. Recall that the state space S usually represents ground-truth information about the agent's environment, which we assume the agent can not directly access. Instead, the agent receives a stream of observations $o \in O$ that convey information about the environment. In this paper, we assume the environment is fully-observable. In other words, the true state can be perfectly inferred from the corresponding observation, given the right feature extractor. The goal of reinforcement learning is to solve for the policy $\pi : O \times A \mapsto [0, 1]$ that maximizes the expected discounted return $\mathcal{J} = \mathbb{E}\left[\sum_{\infty} \gamma^t R(s_t, a_t)\right]$ over infinite horizon, represented as the $Q^{\pi}(o, a)$ function. In this paper, we assume that the policy π consists of an encoder $F : O \mapsto Z$, where Z is a compact latent space, and a policy $\pi_z : Z \times A \mapsto [0, 1]$.

We consider a setting wherein there are two distinct domains: a source domain $\mathcal{M}_{\text{src}}$ and a target domain $\mathcal{M}_{\text{tgt}}$. Crucially, when the agent is placed in the previously unseen target domain, we assume that it can only access its observations and the actions it took, but not reward. Often, we are most interested in the case where shift between $\mathcal{M}_{\text{src}}$ and $\mathcal{M}_{\text{tgt}}$ is induced by differences in the observation spaces O_{src} and O_{tgt}. That is, the state and reward dynamics between the source and target domains are quite similar, but the observation spaces between the two are significantly different. Practically speaking, this can happen quite easily in the presence of distractors, corrupted or malformed inputs, or shifts in sensor readings at test time. Consider a robot that is trained from image observations in a clean environment, and then expected to perform the same task in the wild, where changing lighting conditions and environmental conditions might lead to significantly different image observations. As a result of this distributional shift in the observations on which the policy is conditioned, deploying an agent trained in the source domain directly in the target domain (i.e., zero-shot transfer) results in poor performance.

Given an agent pretrained on a source domain, our goal is to adapt it to the target domain. As we do not have knowledge about the correspondence of observations in the two domains, this setting essentially requires us to make use of unpaired trajectory samples from each domain to drive adaptation. The proposed method, Invariance through Inference, aims to only adapt the encoder F in a manner that minimizes distributional shift in Z between the domains and, in turn, enables the policy π_z to transfer to the unseen target domain, by utilizing only unpaired transitions. We achieve this by jointly optimizing two objectives: *distribution matching* and *dynamics consistency*.

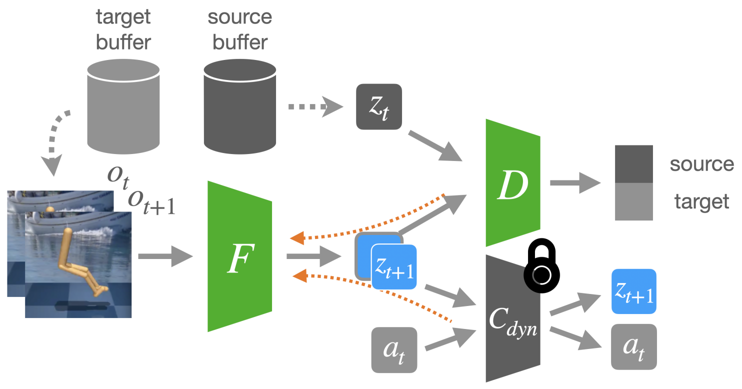

Figure 2: Our proposed Invariance through Inference architecture. The encoder F takes an observation of target domain, and learns to fool the discriminator, while the discriminator D predicts whether the input is an encoded target observation or a latent sample from source buffer. This adversarial training encourages the distribution of encoder outputs to be similar to the latent embedding sampled from the source buffer. C_{dyn} is the pretrained forward and inverse dynamics networks used only to guide the encoder during adaptation.

4 Invariance through Inference

4.1 Distribution Matching

We first deploy a random exploration policy in both the source and target domains to collect samples of observation trajectories

$$\mathcal{B}_{\text{src}} = \left(\ldots, o_t^{\text{src}}, a_t^{\text{src}}, o_{t+1}^{\text{src}}, \ldots\right) \sim P_{\bar{\pi}}(\mathcal{M}_{\text{src}}) \tag{1a}$$
$$\mathcal{B}_{\text{tgt}} = \left(\ldots, o_t^{\text{tgt}}, a_t^{\text{tgt}}, o_{t+1}^{\text{tgt}}, \ldots\right) \sim P_{\bar{\pi}}(\mathcal{M}_{\text{tgt}}), \tag{1b}$$

where $P_{\bar{\pi}}(\mathcal{M})$ denotes the distribution of transitions produced with a random policy in domain $\mathcal{M}$. Given an observation o_t, an encoder F produces a corresponding latent representation z_t

$$z_t^{\text{src}} = F(o_t^{\text{src}}) \tag{2a}$$
$$z_t^{\text{tgt}} = F(o_t^{\text{tgt}}). \tag{2b}$$

We seek to match the distribution over z_t^{tgt} with that over z_t^{src} by adapting the weights of the encoder F, without access to test-time rewards. We employ adversarial training to achieve this. Specifically, our architecture (Fig. 2) includes a discriminator D that tries to distinguish between embeddings from the source domain z_t^{src} and those from the target domain z_t^{tgt}. At the same time, we adapt the parameters of the encoder to produce a latent embedding that is indistinguishable to the discriminator. This results in matching latent distribution over z_t^{src} and z_t^{tgt}. Following the Wasserstein GAN (Arjovsky et al., 2017) formulation, we express our distribution matching loss as

$$\mathcal{J}_{\text{adv}} = \mathbb{E}_{P_{\bar{\pi}}(\mathcal{M}_{\text{src}})}\left[D\left(\bar{F}(o_t^{\text{src}})\right)\right] + \mathbb{E}_{P_{\bar{\pi}}(\mathcal{M}_{\text{tgt}})}\left[1 - D\left(F(o_t^{\text{tgt}})\right)\right], \tag{3}$$

where $\bar{F}$ indicates that the weights of the network are frozen. The encoder tries to minimize this objective while the discriminator acts as an adversary and seeks to maximize it, resulting in a GAN-like minimax game.

4.2 Dynamics consistency

Theoretically, the use of adversarial training can result in an encoder that maps source and target domain observations to latent embeddings that have identical distributions. However, it is possible for a sufficiently expressive encoder to map the same target observations to a random perturbation of observations in the source domain while still matching the distributions (Zhu et al., 2017). To mitigate this, we take advantage of the shared underlying dynamics as a feature-rich and informative source of mutual information between the two domains.

Algorithm 1 Invariance through Inference

```
Require: Pretrained encoder $F$, discriminator $D$, buffers $\mathcal{B}^*_{\text{src}}$ and $\mathcal{B}_{\text{tgt}}$, inverse dynamics network
  parameterized with $\psi_{\text{inv}}$
  for i=1:N do                                                    ▷ Pre-fill buffers
      Sample $z_t, a_t, z_{t+1} \sim P_{\bar{\pi}}(\mathcal{M}_{\text{src}}; F)$
      Sample $o_t, a_t, o_{t+1} \sim P_{\bar{\pi}}(\mathcal{M}_{\text{tgt}})$
      $\mathcal{B}^*_{\text{src}} \leftarrow \mathcal{B}^*_{\text{src}} \cup (z_t, a_t, z_{t+1})$
      $\mathcal{B}_{\text{tgt}} \leftarrow \mathcal{B}_{\text{tgt}} \cup (o_t, a_t, o_{t+1})$
  for $i = 1 : T_{\text{dynamics}}$ do                               ▷ Pretrain dynamics networks
      Sample $z_t, a_t, z_{t+1} \sim \mathcal{B}^*_{\text{src}}$
      $g_{\text{inv}} \leftarrow \nabla_{\psi_{\text{inv}}} \mathcal{L}_{\text{dyn}}(z_t, z_{t+1}, a_t; \psi_{\text{inv}})$
      $\psi_{\text{inv}} \leftarrow \text{Optimizer}(\psi_{\text{inv}}, g_{\text{inv}})$
  for $i = 1 : T_{\text{adapt}}$ do                                  ▷ Adaptation main loop
      Sample $z^{\text{src}}_t, a^{\text{src}}_t, z^{\text{src}}_{t+1} \sim \mathcal{B}^*_{\text{src}}$
      Sample $o^{\text{tgt}}_t, a^{\text{tgt}}_t, o^{\text{tgt}}_{t+1} \sim \mathcal{B}_{\text{tgt}}$
      $g_D \leftarrow \nabla_{\theta_D} \left[D(z^{\text{src}}_t) + (1 - D(F(o^{\text{tgt}}_t)))\right]$      ▷ Distribution matching (adversarial) loss
      $g_{F_1} \leftarrow \nabla_{\theta_F} \left[D(z^{\text{src}}_t) + (1 - D(F(o^{\text{tgt}}_t)))\right]$
      $g_{F_2} \leftarrow \nabla_{\theta_F} \mathcal{L}_{\text{dyn}}(F(o^{\text{tgt}}_t), F(o^{\text{tgt}}_{t+1}), a_t; \psi^*_{\text{inv}})$     ▷ Dynamics consistency loss
      $\theta_D \leftarrow \text{Optimizer}(\theta_D, g_D)$
      $\theta_F \leftarrow \text{Optimizer}(\theta_F, g_{F_1}, g_{F_2})$
```

Specifically, let $C_{\text{inv}}(z_t, z_{t+1}; \psi_{\text{inv}})$ be the inverse dynamics network that predicts the action a_t associated with the transition from z_t to z_{t+1}, and $C_{\text{fwd}}(z_t, a_t; \psi_{\text{fwd}})$ be the forward dynamics network that predicts the next latent $z_{t+1}$from z_t and a_t. We then define the *dynamics consistency loss* as the error in the inverse dynamics predictions

$$\mathcal{L}_{\text{dyn}}(z_t, z_{t+1}, a_t; \psi_{\text{fwd}}, \psi_{\text{inv}}) = \|C_{\text{fwd}}(z_t, a_t; \psi_{\text{fwd}}) - z_{t+1}\|_2^2 + \|C_{\text{inv}}(z_t, z_{t+1}; \psi_{\text{inv}}) - a_t\|_2^2. \quad (4)$$

Most importantly, we pretrain the inverse dynamics network on transitions sampled from the source domain $\mathcal{B}_{\text{src}} \sim P_{\bar{\pi}}(\mathcal{M}_{\text{src}})$ (Eqn. 1a) with observations encoded with F

$$\psi^*_{\text{fwd}}, \psi^*_{\text{inv}} = \underset{\psi_{\text{fwd}}, \psi_{\text{inv}}}{\arg\min}\ \mathbb{E}_{P_{\bar{\pi}}(\mathcal{M}_{\text{src}}; F)} \left[\mathcal{L}_{\text{dyn}}(z^{\text{src}}_t, z^{\text{src}}_{t+1}, a^{\text{src}}_t; \psi_{\text{fwd}}, \psi_{\text{inv}})\right], \quad (5)$$

where $P_{\bar{\pi}}(\mathcal{M}; F)$ is the distribution over latent trajectories. Under the assumption that the underlying dynamics are shared by the domains, we then utilize these learned dynamics models to further encourage the latent embeddings for the target domain to align with those of the source domain. Specifically, during adaptation, we freeze the weights of the forward and inverse dynamics network, and minimize the following dynamics consistency loss with respect to encoder F using transitions sampled from the target domain $\mathcal{B}_{\text{tgt}} \sim P_{\bar{\pi}}(\mathcal{M}_{\text{tgt}})$ (Eqn. 1b)

$$\mathcal{J}_{\text{dyn}} = \mathbb{E}_{P_{\bar{\pi}}(\mathcal{M}_{\text{tgt}}; F)} \left[\mathcal{L}_{\text{dyn}}(z^{\text{tgt}}_t, z^{\text{tgt}}_{t+1}, a^{\text{tgt}}_t; \psi^*_{\text{fwd}}, \psi^*_{\text{inv}})\right]. \quad (6)$$

4.3 Joint Objective

We adapt our encoder by minimizing a loss that combines both the adversarial loss $\mathcal{J}_{\text{adv}}$ (Eqn. 3) and the dynamics consistency loss $\mathcal{J}_{\text{dyn}}$ (Eqn. 6). Specifically, we solve for the parameters of the encoder through the following minimax objective

$$\underset{F}{\arg\min}\ \underset{D}{\arg\max}\ [\mathcal{J}_{\text{adv}} + \mathcal{J}_{\text{dyn}}]. \quad (7)$$

This adaptation objective is effectively maximizing the mutual information between the prototypical representation kept from during training, and the adapted representations of the new observations. Algorithm 1 summarizes the whole procedures to sample trajectory, pretrain dynamics networks and adapt encoder via the objective.

In summary, in contrast to those methods that produce invariance through interpolation, our adaptation objective produce invariance by making statistical inference in the latent space. For this reason we refer to the derived method as Invariance through Inference.

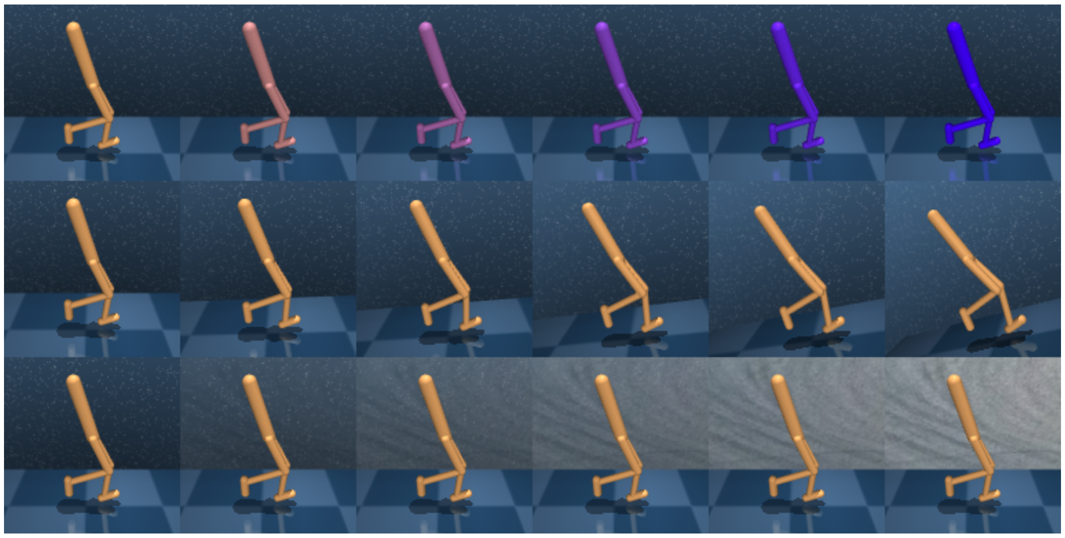

Figure 3: Samples from the modified DistractingCS with intensities increasing from (left-most column) zero to (right-most column) one for the (top row) color, (middle row) camera pose, and (bottom row) background distractions.

5 Experiments

We want to understand the impact of test-time inference on an agent's ability to perform out-of-distribution generalization. This section will compare Invariance through Inference with two state-of-the-art methods for data-augmented reinforcement learning: SVEA (Hansen et al., 2021) and DrQ-v2 (Yarats et al., 2021). Recall from the introduction that these methods vie for increased generalization capabilities by expanding the support of the training distribution. We expect this form of generalization to be less performant than unsupervised adaptation at test time. In our experiments, we will also compare against Policy Adaptation during Deployment (PAD) (Hansen et al., 2020), a baseline that, like our method, adapts the policy without access to the reward at test time.

To further probe the generalization abilities of test-time inference, we conduct an experiment wherein we vary the intensity of environmental distractions. The upshot here is that test-time inference significantly increases the robustness of our policy to distractions during deployment. We will conclude with some general discussion and remarks regarding the design tradeoffs involved in test-time inference.

Setup We conduct experiments using nine domains from the DeepMind Control Suite (DMC) (Tassa et al., 2018). We use DMC as the training (source) environment and the Distracting Control Suite (DistractingCS) (Stone et al., 2021) as the distracted test (target) environment. DistractingCS adds three types of distractions to the DeepMind Control Suite in the form of changes to the background image, deviations in color, and changes to the camera pose relative to training.

Modifications to DistractingCS The default configuration of DistractingCS changes distractions at the start of every episode (e.g., different background images are used at every episode). However, we are interested in measuring an agent's ability to perform inference across several episodes on the same target environment. Thus, we modify DistractingCS to sample a distraction once in the beginning of learning, and then use the same distraction across all learning epochs. This also ensures consistent evaluation across algorithms. In accordance with this change, we also modify the intensity benchmark from DistractingCS. In our experiments, intensity measures the deviation between an environment distraction and the train environment's default value. For example, intensity may measure how far the distracting color is from the default. Finally, we modify the environments to only apply a single distraction during testing (rather than all three) in order to better understand the impact of each type of distraction on overall performance. Figure 3 shows an example of distractions across intensities on Walker-walk domain.

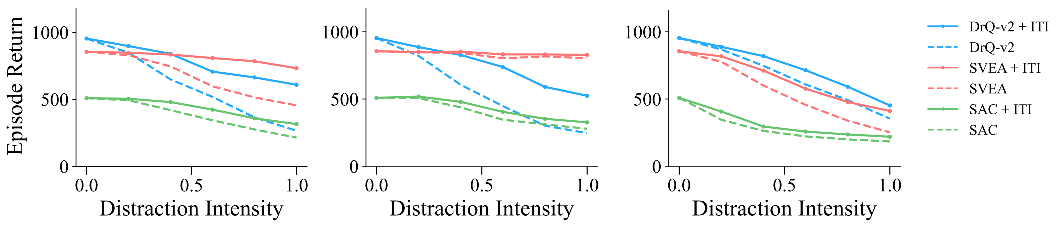

(a) Background (b) Colors (c) Camera Pose

Figure 4: The gain of applying Invariance through Inference to various distracted baselines. Dashed lines denote the performance of the baseline agent in the target environment (i.e., zero-shot), while solid lines represent the performance gains of the base agent with ITI (our method).

5.1 Invariance through Inference On DMControl

This section studies the impact of test-time adaptation on DMControl performance. We begin by pretraining soft actor-critic (SAC) (Haarnoja et al., 2018), SVEA, and DrQ-v2 in a non-distracting training-time environment. After training, we evaluate the learned policies on test environments with distractions of various intensities. This evaluation is zero-shot, i.e., there is no additional training in the test environment.

Table 1: Episode return in the target (test) environments (mean and standard deviation) before (zero-shot) and after (+ITI) adaptation for SAC, SVEA, and DrQ-v2 with background distraction at an intensity setting of 1.0. The performance of each baseline in the source (training) environments can be found in the Appendix.

	SAC		SVEA		DrQ-v2	
Domain	Zero-shot	+ITI	Zero-shot	+ITI	Zero-shot	+ITI
`ball_in_cup-catch`	115 ± 50	$\mathbf{227 \pm 222}$	490 ± 376	$\mathbf{987 \pm 27}$	88 ± 39	$\mathbf{386 \pm 425}$
`cartpole-balance`	434 ± 275	$\mathbf{585 \pm 295}$	446 ± 330	$\mathbf{627 \pm 258}$	273 ± 107	$\mathbf{322 \pm 117}$
`cartpole-swingup`	182 ± 147	$\mathbf{369 \pm 243}$	269 ± 365	$\mathbf{612 \pm 213}$	82 ± 35	$\mathbf{247 \pm 136}$
`cheetah-run`	169 ± 65	$\mathbf{248 \pm 53}$	317 ± 137	$\mathbf{378 \pm 55}$	100 ± 88	$\mathbf{393 \pm 125}$
`finger-spin`	113 ± 162	$\mathbf{192 \pm 196}$	391 ± 467	$\mathbf{943 \pm 54}$	207 ± 328	$\mathbf{769 \pm 206}$
`finger-turn_easy`	$\mathbf{163 \pm 99}$	146 ± 33	278 ± 180	$\mathbf{491 \pm 343}$	268 ± 241	$\mathbf{914 \pm 44}$
`reacher-easy`	179 ± 65	$\mathbf{381 \pm 76}$	75 ± 77	$\mathbf{624 \pm 305}$	58 ± 32	$\mathbf{685 \pm 211}$
`walker-stand`	330 ± 118	$\mathbf{364 \pm 115}$	917 ± 138	$\mathbf{999 \pm 12}$	630 ± 197	$\mathbf{868 \pm 151}$
`walker-walk`	242 ± 142	$\mathbf{291 \pm 134}$	866 ± 45	$\mathbf{924 \pm 45}$	326 ± 195	$\mathbf{770 \pm 140}$

Table 1 presents the results for the different DistractingCS domains in the presence of background distractions with an intensity level of 1.0. Specifically, we compare the test-time performance of SAC, SVEA, and DrQ-v2 in each domain with the episode rewards that we achieve when using our Invariance through Inference algorithm to adapt the encoder. The baseline algorithms employ image augmentation, which provides some robustness to variations at test time. Even then, however, we find that Invariance through Inference adaptation improves the test-time generalization of all three baseline policies in most domains, often resulting in significant performance gains. In cases where Invariance through Inference does not improve performance, the resulting reward is comparable to the baseline policy, i.e., Invariance through Inference does not result in a performance degradation.

Figure 4 visualizes the performance of the different methods, averaged over the set of DistractingCS domains, as a function of the intensity of the distractions. Since the baseline methods are trained with image augmentation, they do exhibit some robustness to distraction. However, we see this robustness rapidly diminishes as the distraction intensity increases. In particular, large changes to camera pose or the image background proved challenging for standard augmentation procedures. Comparatively, Invariance through Inference makes it much smoother and slower degradation of performance. This supports our hypothesis that adaptation powered by unsupervised learning can significantly widen the generalization abilities of learning algorithms.

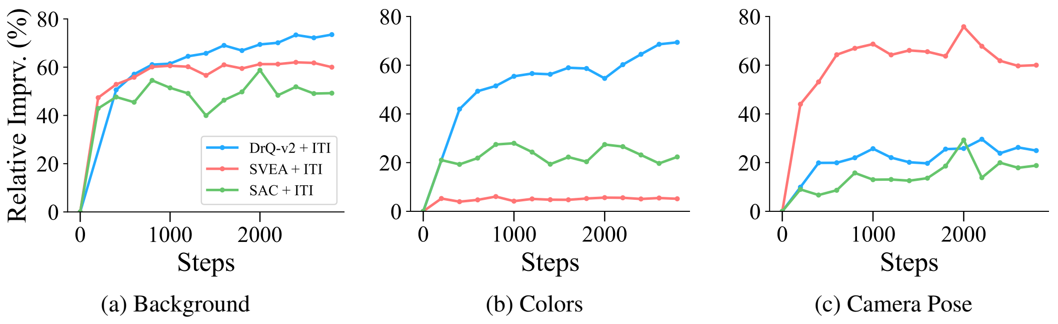

Figure 5: Relative improvement (compared to zero-shot) as a function of adaptation steps when applying ITI to different baseline policies. As in Figure 4, each point represents the mean over nine domains and five random seeds. The results correspond to an intensity value of 1.0.

Table 2: Comparison against PAD

Distraction	Zero-shot	+PAD	+ITI
None	835 ± 230	—	—
Background	213 ± 247	279 ± 271	$\mathbf{425 \pm 292}$
Colors	230 ± 263	271 ± 300	$\mathbf{402 \pm 339}$
Camera Pose	319 ± 265	326 ± 259	$\mathbf{412 \pm 275}$

5.2 Comparisons with PAD

Similar to our approach, PAD pretrains the agent in a clean environment, and then adapts the agent via unsupervised transfer, without assuming access to the target environment's reward function (Hansen et al., 2020). To evaluate the robustness of PAD to distractions, we consider DistractingCS with a fixed distraction intensity of 1.0. Table 2 compares the performance as the difference between the episode returns before and after adaptation along with the episode returns in the clean environment. It should be noted that PAD requires to pretrain a policy along with inverse dynamics prediction objective. Thus we trained SAC with the auxiliary objective specifically for this experiment.

Across all environments, we see that PAD struggles to adapt to distractions at test time. We suspect this instability is caused by the large deviations in the latent variable distribution as a result of changes in the target environment. In particular, we posit that the signal from PAD's inverse dynamics head does not encourage the latent train and test distributions to match, which is a feature specifically baked into Invariance through Inference.

5.3 Further Discussion

Table 3: Ablations with variants of Invariance through Inference that remove inverse, forward dynamics, or adversarial objectives. DrQ-v2 is used as a pretrained policy. We compute episode returns from nine domains and five random seeds, and the results correspond to an intensity value of 1.0.

Distraction	Zero-shot	+ITI	+ITI w/o dyn.	+ITI w/o adv.
Background	228 ± 232	602 ± 300	615 ± 289	176 ± 221
Colors	234 ± 245	536 ± 320	534 ± 327	117 ± 96
Camera Pose	345 ± 287	417 ± 284	407 ± 272	208 ± 235

Ablation Studies In order to better understand the contribution of the different objectives to test-time generalization, we perform a series of ablations in which we omit either the dynamics consistency or the adversarial objectives. In these experiments, we use a pretrained DrQ-v2 network for the algorithm's base policy, and then perform adaptation across all distractions with an intensity value of 1.0. The results in Table 3 show that the adversarial training is critical to adapt the latent representation in the target domain. Performing adaptation using only the dynamics consistency objective, i.e., $\arg\min_F \mathcal{J}_{\text{dyn}}$ (Eqn. 6) results in a significant decrease in performance. We theorize that the dynamics consistency objective helps to refine the local consistency in the latent space when the space in the target domain is close to that of the source domain. If the latent spaces significantly differ, however, we suspect that the gradients may negatively affect convergence.

Compared to the adversarial objective, ablating the dynamics consistency objective has surprisingly little effect on test-time generalization. It may be that the local structure of the latent space is preserved despite the distractions, which then diminishes the net effect of the dynamics consistency objective. For example, one can think of the original points in the latent space simply being shifted and affine-transformed. In this case, solely matching the distributions can effectively undo the transformations, resulting in a representation that is consistent with the original, without the need to explicitly align local structure. We suspect that this may be the case in the domains that we considered, and thus the effect of dynamics consistency objective gets obfuscated.

Pre-Filling the Replay Buffer In our experiments, we pre-filled both the original latent buffer and the target observation buffer with data collected via random exploration. There is nothing particularly special about this choice, random exploration may be subbed out with any exploration strategy. One interesting strategy is to pre-fill the buffer with an exploration strategy that relies on unsupervised pretraining. Given the recent success of these strategies on improving exploration, it seems likely this could further improve performance. We leave this for future work.

6 Closing Remarks

We introduced Invariance through Inference, a new method for leveraging unsupervised data to improve the test-time adaptation of reinforcement learning systems. Empirical results demonstrate that as discrepancies between training and deployment environments become more intense, Invariance through Inference is more capable of adaptation than data augmentation techniques. The problem of test-time adaptation in visual reinforcement learning using unsupervised test-time trajectories is relatively new, but has thus far shown great promise.

Future work in this area might develop better techniques for the initial exploration phase. Many of the environments we considered were quite reversible, with a small intrinsic dimensionality. Expanding this class of methods to work on longer horizon multi-stage tasks is an intriguing possibility.

References

Martin Arjovsky, Soumith Chintala, and Léon Bottou. Wasserstein GAN. *arXiv preprint arXiv:1701.07875*, 2017.

Jimmy Lei Ba, Jamie Ryan Kiros, and Geoffrey E. Hinton. Layer normalization, 2016.

Ting Chen, Simon Kornblith, Mohammad Norouzi, and Geoffrey Hinton. A simple framework for contrastive learning of visual representations. In *Proceedings of the International Conference on Machine Learning (ICML)*, pp. 1597–1607, 2020a.

Xi Chen, Ali Ghadirzadeh, Mårten Björkman, and Patric Jensfelt. Adversarial feature training for generalizable robotic visuomotor control. *Proceedings of the IEEE International Conference on Robotics and Automation (ICRA)*, pp. 1142–1148, 2020b.

Karl Cobbe, Oleg Klimov, Chris Hesse, Taehoon Kim, and John Schulman. Quantifying generalization in reinforcement learning. In *International Conference on Machine Learning*, pp. 1282–1289, 2019.

Yan Duan, John Schulman, Xi Chen, Peter L Bartlett, Ilya Sutskever, and Pieter Abbeel. RL^2: Fast reinforcement learning via slow reinforcement learning. *arXiv preprint arXiv:1611.02779*, 2016.

Chelsea Finn, Pieter Abbeel, and Sergey Levine. Model-agnostic meta-learning for fast adaptation of deep networks. In *Proceedings of the International Conference on Machine Learning (ICML)*, pp. 1126–1135, 2017.

Yaroslav Ganin, Evgeniya Ustinova, Hana Ajakan, Pascal Germain, Hugo Larochelle, François Laviolette, Mario Marchand, and Victor Lempitsky. Domain-adversarial training of neural networks. *Journal of Machine Learning Research*, 17(1):2096–2030, 2016.

Jean-Bastien Grill, Florian Strub, Florent Altché, C. Tallec, Pierre H. Richemond, Elena Buchatskaya, C. Doersch, Bernardo Avila Pires, Zhaohan Daniel Guo, Mohammad Gheshlaghi Azar, B. Piot, K. Kavukcuoglu, Rémi Munos, and Michal Valko. Bootstrap your own latent: A new approach to self-supervised learning. *arXiv preprint arXiv:2006.07733*, 2020.

Tuomas Haarnoja, Aurick Zhou, Kristian Hartikainen, George Tucker, Sehoon Ha, Jie Tan, Vikash Kumar, Henry Zhu, Abhishek Gupta, Pieter Abbeel, and Sergey Levine. Soft actor-critic algorithms and applications. *arXiv preprint arXiv:1812.05905*, 2018.

Danijar Hafner, Timothy Lillicrap, Mohammad Norouzi, and Jimmy Ba. Mastering Atari with discrete world models. *arXiv preprint arXiv:2010.02193*, 2020.

Nicklas Hansen and Xiaolong Wang. Generalization in reinforcement learning by soft data augmentation. *arXiv preprint arXiv:2011.13389*, 2020.

Nicklas Hansen, Rishabh Jangir, Yu Sun, Guillem Alenyà, Pieter Abbeel, Alexei A Efros, Lerrel Pinto, and Xiaolong Wang. Self-supervised policy adaptation during deployment. *arXiv preprint arXiv:2007.04309*, 2020.

Nicklas Hansen, Hao Su, and Xiaolong Wang. Stabilizing deep Q-learning with ConvNets and vision transformers under data augmentation. In *Advances in Neural Information Processing Systems (NeurIPS)*, 2021.

Kaiming He, Haoqi Fan, Yuxin Wu, Saining Xie, and Ross B. Girshick. Momentum contrast for unsupervised visual representation learning. *Proceedings of the IEEE Conference on Computer Vision and Pattern Recognition (CVPR)*, pp. 9726–9735, 2020.

Rein Houthooft, Richard Y Chen, Phillip Isola, Bradly C Stadie, Filip Wolski, Jonathan Ho, and Pieter Abbeel. Evolved policy gradients. *arXiv preprint arXiv:1802.04821*, 2018.

Kyle Hsu, Sergey Levine, and Chelsea Finn. Unsupervised learning via meta-learning. *arXiv preprint arXiv:1810.02334*, 2018.

Max Jaderberg, Volodymyr Mnih, Wojciech Marian Czarnecki, Tom Schaul, Joel Z Leibo, David Silver, and Koray Kavukcuoglu. Reinforcement learning with unsupervised auxiliary tasks. *arXiv preprint arXiv:1611.05397*, 2016.

Aviral Kumar, Rishabh Agarwal, Aaron Courville, Tengyu Ma, George Tucker, and Sergey Levine. Value-based deep reinforcement learning requires explicit regularization. In *ICML 2021 Reinforcement Learning for Real Life Workshop*, 2021.

Michael Laskin, Kimin Lee, Adam Stooke, Lerrel Pinto, Pieter Abbeel, and Aravind Srinivas. Reinforcement learning with augmented data. *arXiv preprint arXiv:2004.14990*, 2020.

Kimin Lee, Kibok Lee, Jinwoo Shin, and Honglak Lee. A simple randomization technique for generalization in deep reinforcement learning. *arXiv preprint arXiv:1910.05396*, 2019.

Xue Bin Peng, Marcin Andrychowicz, Wojciech Zaremba, and Pieter Abbeel. Sim-to-real transfer of robotic control with dynamics randomization. In *Proceedings of the IEEE International Conference on Robotics and Automation (ICRA)*, May 2018.

Martin L Puterman. *Markov Decision Processes: Discrete Stochastic Dynamic Programming*. John Wiley & Sons, August 2014.

Roberta Raileanu, Max Goldstein, Denis Yarats, Ilya Kostrikov, and Rob Fergus. Automatic data augmentation for generalization in deep reinforcement learning. *arXiv preprint arXiv:2006.12862*, 2020.

Kate Rakelly, Aurick Zhou, Chelsea Finn, Sergey Levine, and Deirdre Quillen. Efficient off-policy meta-reinforcement learning via probabilistic context variables. In *Proceedings of the International Conference on Machine Learning (ICML)*, pp. 5331–5340, 2019.

Jonas Rothfuss, Dennis Lee, Ignasi Clavera, Tamim Asfour, and Pieter Abbeel. ProMP: Proximal meta-policy search. *arXiv preprint arXiv:1810.06784*, 2018.

Max Schwarzer, Ankesh Anand, Rishab Goel, R Devon Hjelm, Aaron Courville, and Philip Bachman. Data-efficient reinforcement learning with momentum predictive representations. *arXiv preprint arXiv:2007.05929*, 2020.

Laura Smith, Nikita Dhawan, Marvin Zhang, Pieter Abbeel, and Sergey Levine. AVID: Learning multi-stage tasks via pixel-level translation of human videos. *arXiv preprint arXiv:1912.04443*, 2019.

Aravind Srinivas, Michael Laskin, and Pieter Abbeel. Curl: Contrastive unsupervised representations for reinforcement learning. *arXiv preprint arXiv:2004.04136*, 2020.

Bradly C Stadie, Pieter Abbeel, and Ilya Sutskever. Third-person imitation learning. *arXiv preprint arXiv:1703.01703*, 2017.

Austin Stone, Oscar Ramirez, Kurt Konolige, and Rico Jonschkowski. The distracting control suite—A challenging benchmark for reinforcement learning from pixels. *arXiv preprint arXiv:2101.02722*, 2021.

Yuval Tassa, Yotam Doron, Alistair Muldal, Tom Erez, Yazhe Li, Diego de Las Casas, David Budden, Abbas Abdolmaleki, Josh Merel, Andrew Lefrancq, Timothy Lillicrap, and Martin Riedmiller. DeepMind Control Suite. *arXiv preprint arXiv:1801.00690*, 2018.

Dequan Wang, Evan Shelhamer, Shaoteng Liu, Bruno Olshausen, and Trevor Darrell. Tent: Fully test-time adaptation by entropy minimization. *arXiv preprint arXiv:2006.10726*, 2020.

Denis Yarats, Rob Fergus, Alessandro Lazaric, and Lerrel Pinto. Mastering visual continuous control: Improved data-augmented reinforcement learning. *arXiv preprint arXiv:2107.09645*, 2021.

Amy Zhang, Nicolas Ballas, and Joelle Pineau. A dissection of overfitting and generalization in continuous reinforcement learning. *arXiv preprint arXiv:1806.07937*, 2018.

Qiang Zhang, Tete Xiao, Alexei A. Efros, Lerrel Pinto, and Xiaolong Wang. Learning cross-domain correspondence for control with dynamics cycle-consistency. *arXiv preprint arXiv:2012.09811*, 2020.

Jun-Yan Zhu, Taesung Park, Phillip Isola, and Alexei A Efros. Unpaired image-to-image translation using cycle-consistent adversarial networks. In *Proceedings of the IEEE Conference on Computer Vision and Pattern Recognition (CVPR)*, pp. 2223–2232, 2017.

A Appendix

The following provide a more detailed experimental evaluation of Invariance through Inference on the Distracting Control Suite.

B Performance in original domains

Table 4 presents the average reward for the baseline SAC, SVEA, and DrQ-v2 on the non-distracted source domains. The method labeled SAC+Inv denotes a soft actor-critic agent that is trained using inverse dynamics as an additional auxiliary objective that is only used in making a comparison against PAD.

Table 4: Performance in the original (clean) domains.

Domain	SAC	SAC+Inv	SVEA	DrQ-v2
`ball_in_cup-catch`	452 ± 303	999 ± 7	1007 ± 4	1007 ± 3
`cartpole-balance`	1022 ± 8	988 ± 26	996 ± 21	969 ± 123
`cartpole-swingup`	735 ± 167	885 ± 24	892 ± 15	874 ± 21
`cheetah-run`	309 ± 26	415 ± 59	448 ± 105	897 ± 45
`finger-spin`	615 ± 63	971 ± 64	1000 ± 37	997 ± 36
`finger-turn_easy`	138 ± 28	658 ± 141	539 ± 317	945 ± 46
`reacher-easy`	381 ± 39	723 ± 383	812 ± 293	988 ± 28
`walker-stand`	438 ± 111	997 ± 6	1006 ± 4	996 ± 31
`walker-walk`	393 ± 117	915 ± 22	964 ± 34	980 ± 16

C Ablations

Tables 5, 6, and 7 provide a per-domain ablation summary for background, color, and camera pose distractions, respectively. As with the results in Table 3, we use DrQ-v2 as the pretrained policy and present the mean reward and standard deviation for five random seeds.

Table 5: Ablation with Background distraction

Domain	Zero-shot	+ITI	+ITI w/o inv., fwd.	+ITI w/o inv.	+ITI w/o fwd.	+ITI w/o adv.
`walker-walk`	326 ± 196	749 ± 133	778 ± 142	777 ± 145	768 ± 146	268 ± 367
`walker-stand`	623 ± 233	866 ± 153	883 ± 110	859 ± 144	873 ± 129	402 ± 347
`cartpole-swingup`	82 ± 35	231 ± 128	395 ± 218	288 ± 163	246 ± 152	117 ± 43
`ball_in_cup-catch`	88 ± 39	394 ± 387	381 ± 416	400 ± 414	383 ± 381	93 ± 42
`finger-spin`	208 ± 327	783 ± 214	742 ± 190	772 ± 225	769 ± 223	74 ± 160
`reacher-easy`	98 ± 93	726 ± 149	713 ± 111	732 ± 104	694 ± 169	91 ± 54
`cheetah-run`	98 ± 90	411 ± 191	397 ± 152	398 ± 147	419 ± 157	12 ± 19
`cartpole-balance`	271 ± 101	336 ± 126	315 ± 98	367 ± 84	297 ± 121	264 ± 80
`finger-turn_easy`	261 ± 244	920 ± 41	929 ± 57	899 ± 52	909 ± 74	256 ± 264

D Architectures

This section describes the architectures of encoder F, discriminator D, inverse dynamics C_{inv} and forward dynamics C_{fwd}. Encoder architectures follow the originally presented design choices of each base policy except for DrQ-v2. We take the part of the original network that produces a latent for the actor, and use it as an encoder F. In all of SAC (of the version used in (Hansen et al., 2021)), SVEA and PAD, this shared latent is set to have dimension 100. For DrQ-v2, we took the entire network architecture from SVEA. The discriminator consists of a linear layer with hidden dimension 100 followed by Layer Normalization (LN) (Ba et al., 2016) and tanh activation, and a three layer

Table 6: Ablation with Color distraction

Domain	Zero-shot	+ITI	+ITI w/o inv., fwd.	+ITI w/o inv.	+ITI w/o fwd.	+ITI w/o adv.
`walker-walk`	80 ± 43	481 ± 313	468 ± 305	495 ± 330	472 ± 319	26 ± 5
`walker-stand`	278 ± 150	543 ± 231	603 ± 283	571 ± 259	548 ± 268	145 ± 31
`cartpole-swingup`	152 ± 84	552 ± 377	520 ± 359	507 ± 339	434 ± 395	94 ± 56
`ball_in_cup-catch`	239 ± 374	812 ± 225	857 ± 182	840 ± 251	843 ± 196	131 ± 46
`finger-spin`	349 ± 354	612 ± 345	561 ± 376	591 ± 351	603 ± 358	143 ± 172
`reacher-easy`	138 ± 135	490 ± 416	486 ± 392	486 ± 362	445 ± 405	140 ± 90
`cheetah-run`	193 ± 188	422 ± 282	416 ± 293	421 ± 277	406 ± 285	4 ± 2
`cartpole-balance`	481 ± 351	602 ± 366	576 ± 359	593 ± 351	583 ± 349	216 ± 94
`finger-turn_easy`	194 ± 200	313 ± 290	323 ± 337	297 ± 316	304 ± 323	170 ± 57

Table 7: Ablation with Camera Pose distraction

Domain	Zero-shot	+ITI	+ITI w/o inv., fwd.	+ITI w/o inv.	+ITI w/o fwd.	+ITI w/o adv.
`walker-walk`	293 ± 195	375 ± 154	369 ± 168	389 ± 161	366 ± 164	63 ± 71
`walker-stand`	621 ± 202	704 ± 105	617 ± 155	661 ± 146	679 ± 93	330 ± 252
`cartpole-swingup`	286 ± 51	234 ± 123	211 ± 122	241 ± 140	281 ± 42	172 ± 132
`ball_in_cup-catch`	327 ± 227	462 ± 307	429 ± 321	566 ± 314	400 ± 337	199 ± 169
`finger-spin`	29 ± 25	252 ± 216	222 ± 209	275 ± 194	251 ± 206	32 ± 63
`reacher-easy`	917 ± 101	933 ± 47	925 ± 60	950 ± 72	940 ± 90	732 ± 159
`cheetah-run`	55 ± 20	142 ± 57	154 ± 90	141 ± 74	144 ± 61	24 ± 28
`cartpole-balance`	288 ± 46	307 ± 100	375 ± 83	379 ± 116	380 ± 64	217 ± 47
`finger-turn_easy`	287 ± 89	346 ± 219	359 ± 122	377 ± 200	421 ± 180	160 ± 97

multi-layer perceptron (MLP) with and ReLU activations. Inverse dynamics network C_{inv} is five layer MLP and ReLU activations. It takes the concatenated latents as its input. Forward dynamics network C_{fwd} takes action and latent, and encode them separately followed by concatenation and further layers. The action is fed it to a linear layer followed by LN, another linear layer and ReLU with hidden dimension 100. The latent is fed to three layer MLP where the first activation is LN and others are ReLU. The both encoded inputs are concatenated and fed to 4 layer MLP with ReLU activations followed by LN and tanh activation. In all layers except for those explicitly mentioned, hidden dimension is set to $1,024$.

E HYPERPARAMETERS

This section details the hyperparameter settings that were used for the experimental evaluation. The hyperparameters relevant to pretraining dynamics network are listed in Table 8, and those relevant to adaptation are listed in Table 9. For the base policies, we followed the hyperparameters and architecture choices on their original paper. Those information on SAC and SVEA can be found in (Hansen et al., 2021), and PAD in (Hansen et al., 2020). The dimension of the latent z_t differs depending on the encoder of the base policy, but all of the encoders in our experiments produce a latent with dimension 100.

Table 8: Hyperparameters for dynamics pretraining

Hyperparameter	Value
Steps (T_{dyn})	$100,000$
Batch size	256
Optimizer	RMSProp($\alpha = 0.99, \epsilon = 1.0 \times 10^{-8}$)
Learning rate (forward dynamics)	0.001
Learning rate (inverse dynamics)	0.001

Table 9: Hyperparameters for adaptation

Hyperparameter	Value
Capacity of buffers (N_{buf})	$1,000,000$
Batch size	256
Discriminator updates per step	5
Gradient clipping	0.01
Optimizer	RMSProp($\alpha = 0.99, \epsilon = 1.0 \times 10^{-8}$)
Learning rate (encoder)	1.0×10^{-4} (for DrQ-v2)
	1.0×10^{-5} (otherwise)
Learning rate (discriminator)	1.0×10^{-4} (for DrQ-v2)
	1.0×10^{-5} (otherwise)
Learning rate (inverse dynamics)	1.0×10^{-6}